



OPEN

Influence of thermocycling on the antifungal properties of 3D printed denture base material containing zwitterionic and quaternary ammonium compounds

Sae-Eun Lee^{1,2} & Jae-Sung Kwon^{1,2}✉

Denture stomatitis, primarily caused by the colonization of *Candida albicans* biofilms, remains a persistent clinical challenge. This study investigated the effects of incorporating 2-methacryloyloxyethyl phosphorylcholine (MPC) and dimethyl dioctadecyl ammonium bromide (DDAM) into 3D-printed denture base resins to enhance their antifungal properties and evaluate their impact on flexural strength, even after undergoing thermocycling. Following simulated thermal aging (10,000 thermal cycles), all groups exhibited a decline in antifungal efficacy, with the most pronounced reduction observed in the 2% DDAM group. Notably, statistical analysis confirmed significant differences between before- and after-aging states, highlighting the impact of thermal aging on antifungal performance. In contrast, the flexural strength was better maintained in the MPC group, whereas an optimal balance between antifungal efficacy and mechanical performance was achieved in the combination group (1% MPC + 1% DDAM). Thermocycling demonstrated the long-term durability of the experimental resins, with a slight decline in antifungal activity over time. This study highlights the potential of MPC and DDAM as functional additives to enhance the antifungal properties of 3D-printed denture base resins while maintaining acceptable flexural strength, offering a promising strategy for addressing denture stomatitis.

Keywords Zwitterionic, Quaternary ammonium compounds, PMMA, Denture base resin, Antifungal property, Mechanical property

Medical technology advancements and expertise have significantly increased human life expectancy, resulting in a growing aging population¹. Consequently, the increased prevalence of complete edentulism has posed a critical global health concern². Removable full dentures remain the standard treatment for patients with complete edentulism³. Poly methyl methacrylate (PMMA) has been the material of choice for denture base materials over the past few years due to its favorable properties, including biocompatibility, esthetic appeal, versatility, low cost, and ease of fabrication^{4,5}. However, despite these advantages, the poor antimicrobial properties of PMMA have been considered a notable limitation, which increases the risk of oral infections and the development of unpleasant odors⁶.

Previous studies have reported that a significant proportion of denture wearers experience denture stomatitis, a fungal infection predominantly caused by *Candida albicans*⁷. This infection is exacerbated by microbial adhesion to the denture surfaces⁸. Various methods have been proposed to mitigate these issues, including the use of denture cleansers and the incorporation of antifungal agents into denture base materials⁹. However, these approaches have limitations, such as altering the denture surface properties, increasing roughness, and potentially contributing to the development of drug resistance¹⁰. Moreover, the frequent use of antifungal medications increases the risk of developing drug resistance¹¹. Modifying denture materials is a promising alternative to prevent microbial adhesion¹². Materials such as 2-methacryloyloxyethyl phosphorylcholine (MPC), a hydrophilic and biocompatible polymer, have demonstrated protein-repelling properties and reduced microbial adhesion when incorporated into denture resins^{13–15}. Furthermore, quaternary ammonium compounds (QAMs), a class

¹Department and Research Institute of Dental Biomaterials and Bioengineering, Yonsei University College of Dentistry, 50-1 Yonsei-ro, Seodaemun-gu, Seoul 03722, Republic of Korea. ²BK21 FOUR Project, Yonsei University College of Dentistry, 50-1 Yonsei-ro, Seodaemun-gu, Seoul 03722, Republic of Korea. ✉email: JK WON@yuhs.ac

of antibacterial agents, have gained attention for their ability to combat oral pathogens¹⁶. These compounds can be immobilized within resin matrices, providing long-lasting, contact-based antimicrobial effects without leaching¹⁷.

Although several previous studies have explored the mechanical properties and antifungal efficacy of three-dimensional 3D-printed denture base materials, few have investigated the effects of both MPC and DDAM incorporation, particularly in comparison to each other. Furthermore, no studies have evaluated the longevity of these properties after thermocycling. By addressing these gaps, this study provides valuable insights into the sustained antifungal performance and mechanical stability of these materials over time.

This study aimed to develop an antifungal 3D-printed denture base material by incorporating MPC, a protein-repellent agent, and dimethyl dioctadecyl ammonium bromide (DDAM), an antifungal agent to prevent *C. albicans* adhesion. The following null hypotheses were tested: (1) between 3D-printed denture base resins containing MPC and those containing DDAM, there would be no significant differences in the antifungal efficacy or flexural strength and (2) even after thermocycling, the antifungal efficacy and flexural strength of 3D-printed denture base resin containing MPC and DDAM would not show significant differences.

Materials and methods

Materials

A commercial 3D printable PMMA material for denture (NextDent Denture 3D+; 3D Systems, Soesterberg, Netherlands) in a light pink hue (LOT:WW251N04) was used to manufacture the denture base resin used in this study. The resin was used as the carrier for the protein-repellent monomer MPC and the antifungal agent DDAM. MPC and DDAM were purchased from Sigma-Aldrich (St. Louis, MO, USA) and used without further purification.

Formulation of the 3D-printed denture base resin incorporated with MPC and/or DDAM

The preparation process involved dissolving MPC and DDAM powders in ethanol at a 1:4 ratio, followed by sonication at 40% amplitude for 20 min (Q500 sonicator, Qsonica, USA). The mixture was stirred at 800 rpm at 50 °C for 48 h to ensure homogeneous dispersion of the additives. Degassing was performed under vacuum (7–8 mTorr) for 2 h. A schematic illustration of the mixing and printing protocol is shown in Fig. 1. Specimens were fabricated using the NextDent 5100 3D printer (NextDent, 3D Systems, Netherlands) with a 50 µm layer thickness, followed by UV post-curing at 350–500 nm for 30 min. Before antifungal testing, all specimens were sterilized using an ethylene oxide (EO) gas sterilizer according to the manufacturer's instructions.

A digital balance (XS105, Metter-toledo AG, Greifensee, Switzerland) was used to weigh the PMMA, which was then mixed with MPC and DDAM at a mass ratio of 2.0 wt%. The detailed filler content of the experimental group is listed in Table 1. For 3D printing, cylindrical specimens measuring 10 × 2 mm were sketched using Exocad Dental CAD software (version 3.2 Elefsina, build 9036, exocad GmbH, Darmstadt, Germany; <http://www.exocad.com>). Post-printing, the specimens were washed with isopropanol to remove any remaining denture resin and stored for further post-curing in a high-performance photocuring unit (Next Dent LC-3D print box, 3D systems, Soesterbeg, The Netherlands) at 350–500 nm ultraviolet light for 30 min.

Fourier-transform infrared spectroscopy (FT-IR)

Fourier-transform infrared spectroscopy (FT-IR, INVENIO, Bruker, Billerica, MA, USA) analysis was performed to characterize the chemical composition of the MPC and DDAM powders and to analyze 3D-printed denture

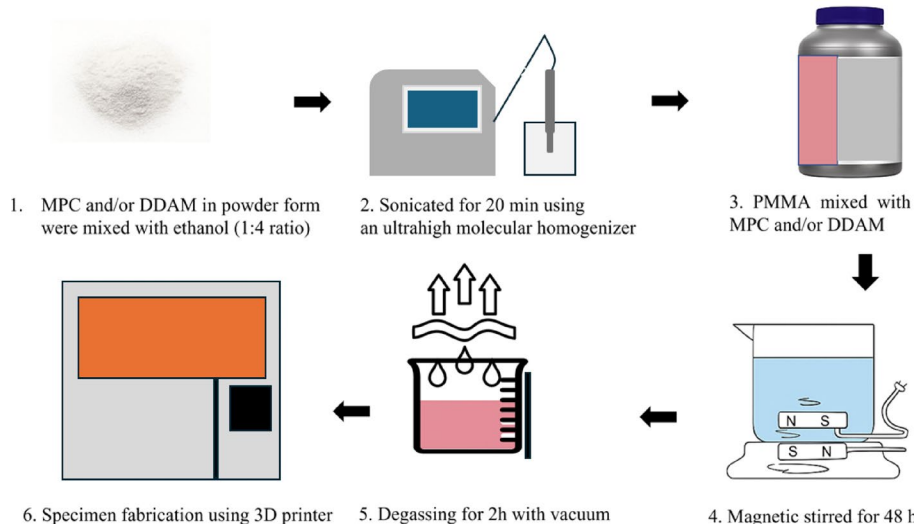


Fig. 1. Demonstration of the preparation process of 3D-printed denture base resin incorporating MPC and/or DDAM.

Groups	PMMA (wt%)	MPC (wt%)	DDAM (wt%)
Control	100	-	-
2% MPC	98	2	-
2% DDAM	98	-	2
1% MPC + 1% DDAM	98	1	1

Table 1. The weight percentage of MPC and/or DDAM based on the 3D-printed denture base resin content in the sample group.

base resin specimens in four groups: control, 2% MPC, 2% DDAM, and 1% MPC + 1% DDAM. Spectra were collected in the range of 400 to 2000 cm^{-1} and analyzed using the IR Lab Solution OPUS software (Version 8.5, Bruker Optik GmbH, Ettlingen, Germany; <https://www.bruker.com/en/products-and-solutions/infrared-and-raman/opus-spectroscopy-software.html>).

The thermocycling procedure

Specimens were divided into two groups: one without thermocycling and the other subjected to 10,000 cycles in distilled water between 5 and 55 °C with a dwell time of 30 s at each temperature, using thermocycling machine (ThermoCycling Tester, R&B Inc., Daejeon, Korea). For the CFU test, specimens were evaluated before ($n=3$) and after ($n=3$) thermocycling. For the flexural strength test, specimens were evaluated before ($n=5$) and after ($n=5$) thermocycling in each of the four groups. For the CLSM analysis, specimens were evaluated before ($n=1$) and after ($n=1$) thermocycling.

Colony forming units (CFU)

C. albicans (ATCC 10231) were used to evaluate the antifungal effects of the 3D-printed denture base resin incorporated with MPC and DDAM. Frozen *C. albicans* colonies were thawed and cultured in Sabouraud dextrose broth (SD broth; MBcell, Seoul, Korea) at 37 °C for 24 h. The fungi were further cultivated by inoculating an isolated colony into the SD broth and incubating at 37 °C for 24 h. The culture was then diluted with SD broth to prepare a *C. albicans* suspension with a concentration of approximately 1×10^6 CFU/ml.

For the CFU test, disc-shaped specimens were fabricated with dimensions of 10 mm in diameter and 2 mm in thickness. For each group, three specimens before thermocycling ($n=3$) and three after thermocycling ($n=3$) were used. The test was performed in three replicates, resulting in a total of 72 specimens across all four groups. Prior to the CFU test, all specimens were sterilized using an ethylene oxide (EO) gas sterilizer according to the manufacturer's protocol. After dilution to approximately 1×10^6 CFU/mL, 1 mL of the *C. albicans* suspension was placed onto each sterilized specimen and incubated in a 24-well plate at 37 °C for 24 h to allow biofilm formation under static conditions.

Confocal laser scanning microscopy (CLSM) analysis

CLSM was used to analyze *C. albicans* attached to the specimens. For each group, one specimen before ($n=1$) and one after ($n=1$) thermocycling were examined, resulting in a total of eight specimens across all four groups. After washing with phosphate-buffered saline (PBS) to remove non-attached fungus, the specimens with attached fungus were stained using the "LIVE/DEAD" Yeast Viability Kit (SYTO 9 and propidium iodide, Molecular Probes, Engene, OF, USA) for 30 min. The specimens were then rinsed with PBS and observed under 20× magnification using a confocal microscope (LSM 980, Carl Zeiss, Thornwood, NY, USA).

Flexural strength

The flexural strength was evaluated according to ISO 20,795–1. Rectangular bar-shaped specimens were printed with dimensions of 64 mm in length, 10 mm in width, and 3.3 mm in height. A total of 40 specimens were used for the test—five specimens before thermocycling ($n=5$) and five after thermocycling ($n=5$) for each of the four groups. The specimens were then stored in distilled water at (37 ± 1) °C for (50 ± 2) h. After conditioning, the specimens were tested using a universal testing machine (Instron 5942, Norwood, MA, USA), with a 1 kN load applied at a crosshead speed of 5 mm/min. The flexural strength (σ) was calculated using the following equation:

$$\sigma = \frac{3Fl}{2bh^2} \quad (1)$$

where F denotes the maximum load applied to the specimen (N), l is the distance between the supports (50 mm), and b and h are the width and height (mm) of the specimen.

Statistical analysis

Statistical analysis was conducted using IBM SPSS Statistics 28.0 software (IBM, Armonk, NY, USA). All data were tested for homogeneity using Levene's test, One-way analysis of variance (ANOVA) followed by Tukey's post hoc test was conducted to compare differences among the experimental groups. In addition, paired t-tests were performed to evaluate the differences between pre-aging and post-aging conditions within each group for both flexural strength and CFU. A p value of < 0.05 was considered statistically significant.

Results

FT-IR

FT-IR spectroscopy was performed to analyze potential chemical interactions between the control resin (PMMA 100%) and specimens containing 2% MPC, 2% DDAM, or a combination of both (1% MPC + 1% DDAM). The analysis focused on identifying changes in peak intensities and positions, particularly around the characteristic absorption bands such as $\sim 1720\text{ cm}^{-1}$ (C=O), $\sim 2950\text{ cm}^{-1}$ (C-H), and 1000–1500 cm^{-1} (C-C-O and C-N), which indicate possible bond formation or molecular interactions between the polymer matrix and incorporated agents. The resulting spectra were compared to identify any structural changes induced by the additives (Fig. 2).

In the control group, characteristic PMMA peaks were observed, including a strong ester carbonyl (C=O) stretching band near 1720 cm^{-1} , C-O-C asymmetric stretching in the range of 1140–1190 cm^{-1} , and C-H stretching vibrations around 2950 cm^{-1} .

Upon the incorporation of MPC, subtle changes in peak intensity and position, particularly around 1720 cm^{-1} , were observed. These alterations suggest potential interactions between the ester groups in MPC and the PMMA matrix. Additionally, new or enhanced vibrational modes in the 1000–1500 cm^{-1} region may reflect the introduction of phosphate-containing functionalities from MPC.

Similarly, the incorporation of DDAM significantly altered the spectral profile in both the 1720 cm^{-1} and 1000–1500 cm^{-1} regions, which is likely attributable to the presence of amine or quaternary ammonium functional groups.

When both MPC and DDAM were incorporated (MPC+DDAM), the spectrum exhibited more complex changes in the same characteristic regions. These findings suggest that MPC and DDAM not only interact with PMMA but may also influence each other's incorporation, potentially leading to synergistic effects or the formation of new chemical linkages.

Overall, FT-IR analysis confirms that the incorporation of MPC, DDAM, and their combination induces measurable chemical changes in the PMMA matrix, likely due to molecular interactions and bond formation between the additives and the resin.

CFU

The colony forming units (CFU) of *C. albicans* attached to the specimen surface are presented in Fig. 3. The CFU were highest in the control group both before- and after-aging. Compared with the control group, the 2% MPC, 2% DDAM, and 1% MPC + 1% DDAM groups exhibited significantly lower CFU ($p < 0.05$). Among these, the combination group (1% MPC + 1% DDAM) showed the lowest CFU both before- and after-aging. Following thermocycling (10,000 cycles), paired t-test analysis revealed significant increases in CFU for the control ($p = 0.014$), 2% MPC ($p = 0.001$), 2% DDAM ($p = 0.003$), and 1% MPC + 1% DDAM ($p = 0.003$) groups, indicating reduced antifungal performance after-aging. Nevertheless, despite the overall decrease in antifungal activity, the 1% MPC + 1% DDAM group consistently maintained the lowest CFU, demonstrating superior durability and antifungal effectiveness compared to the other groups.

CLSM analysis

Additionally, CLSM images obtained after thermocycling demonstrated that antifungal effects were retained even after-aging (Fig. 4). In the Live/Dead assay, a large number of fungi were observed in the control group, whereas a relatively small number of live fungal cells were observed in all experimental groups. The results revealed that integrating MPC and DDAM not only reduced the attachment of fungi compared to the control group but also killed them on contact.

Flexural strength

The flexural strength of the control and experimental groups (2% MPC, 2% DDAM, and 1% MPC + 1% DDAM) was evaluated before- and after-aging, as shown in the graph (Fig. 5). The flexural strength values of the MPC and DDAM groups varied compared to the control group. Before-aging, the control group exhibited the highest flexural strength, while the 2% DDAM group showed the lowest values. After-aging, a significant reduction in flexural strength was observed in the 2% MPC ($p = 0.035$) and 2% DDAM groups ($p = 0.021$), whereas no

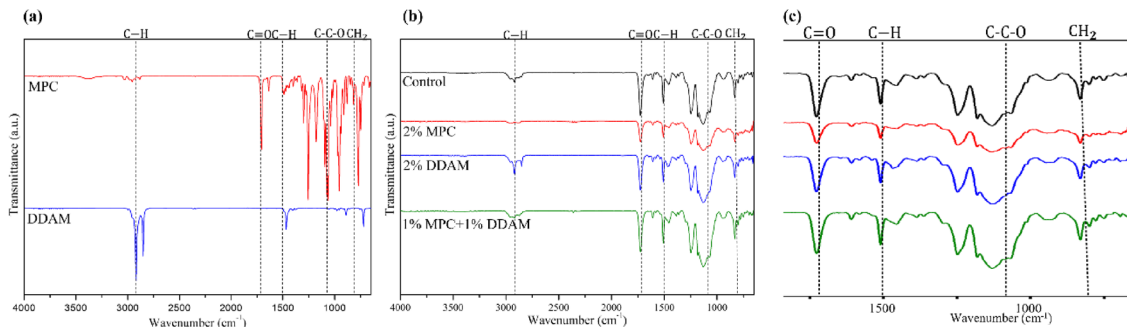


Fig. 2. FT-IR analysis (a) Powder MPC and DDAM. (b) 3D-printed denture base resin incorporating MPC and/or DDAM. (c) Enlarged view of the characteristic regions ($\sim 1720\text{ cm}^{-1}$ and 1000–1500 cm^{-1}) highlighting subtle intensity changes and chemical interactions with the PMMA matrix.

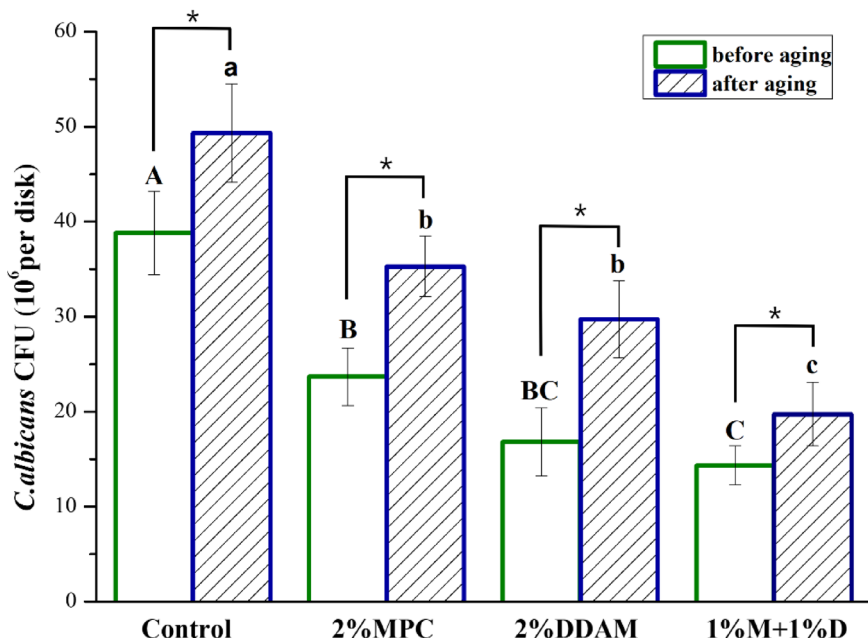


Fig. 3. Effects of MPC and DDAM on *C. albicans* CFU (10^6 per disk). The bars with capital letters reveal significant differences between the before-aging groups, and the lowercase letters indicate significant differences between the after-aging groups ($p < 0.05$). Asterisks (*) indicate statistically significant differences between the before- and after-aging conditions within each group (paired t-test, $p < 0.05$).

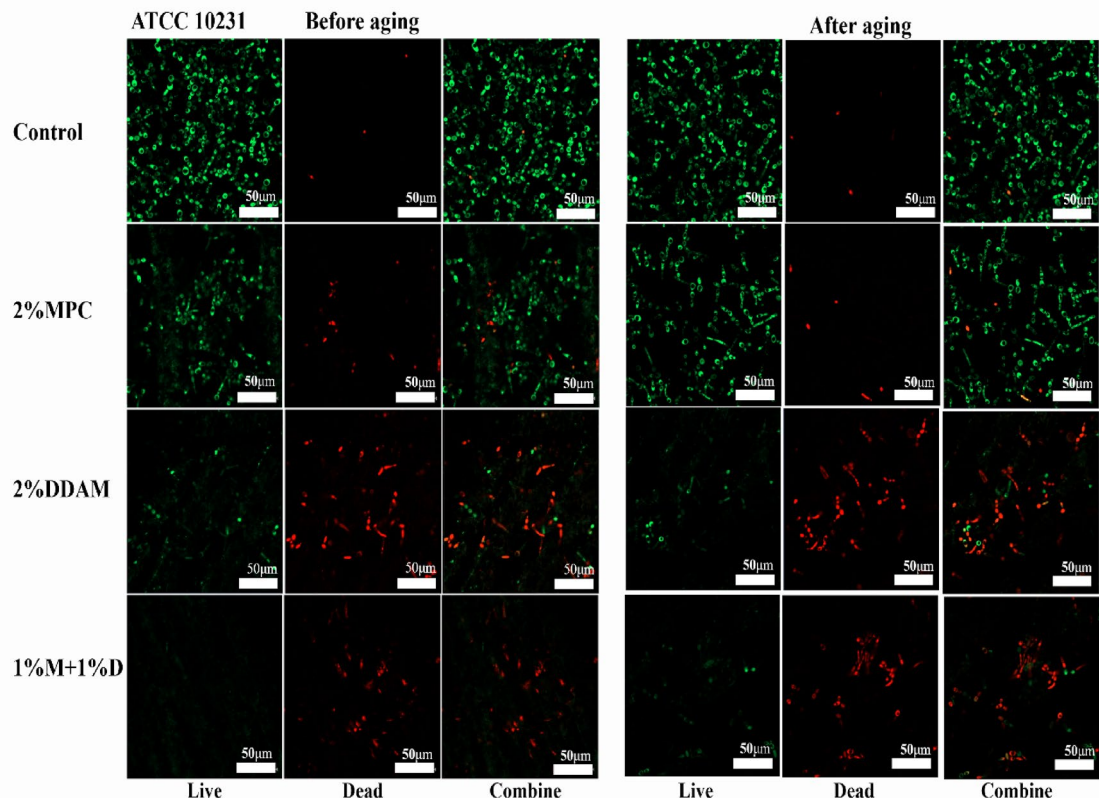


Fig. 4. Confocal laser scanning microscope (CLSM) images for the Live/Dead viability testing of each fabricated specimen before- and after-aging. Green indicates live cells and red indicates dead cells. The scale for all images shown was 50 μ m.

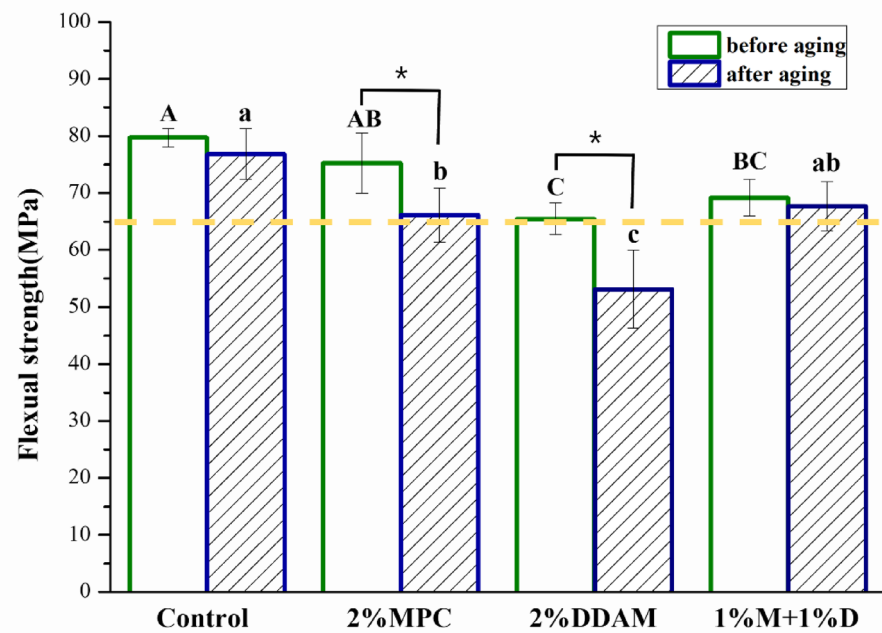


Fig. 5. Flexural strength of the 3D-printed denture base resin. Horizontal dotted lines (yellow) indicate the minimum requirement for the denture base resin in accordance to ISO 20,795-1. The bars with capital letters denote significant differences between the before-aging groups, and the lowercase letters indicate significant differences between the after-aging groups ($p < 0.05$). Asterisks (*) represent significant differences between the before- and after-aging conditions within the same based on paired t-test ($p < 0.05$).

significant changes were found in the control ($p = 0.210$) and MPC+DDAM groups ($p = 0.525$). Among the after-aging conditions, the MPC+DDAM group demonstrated intermediate flexural strength (67.68 MPa), which was statistically comparable to the control. The MPC-only group maintained higher flexural strength compared to the DDAM group, indicating a more favorable balance between strength and biofunctionality. With the exception of the after-aging 2% DDAM group, all groups satisfied the ISO 20,795-1 minimum requirement of 65 MPa for denture base resins.

Discussion

Although a formal power analysis was not performed, the sample sizes were determined based on previous similar studies, and were deemed sufficient to detect significant differences.

FT-IR analysis indicated minor chemical interactions between MPC/DDAM and the PMMA matrix, possibly explaining the slight reductions in flexural strength due to network alterations.

Future work will explore varying concentrations and ratios of MPC and DDAM incorporation to optimize both antifungal efficacy and mechanical properties.

The effects of adding MPC and DDAM to a 3D-printed denture base resin were analyzed in this study. The results rejected the first null hypothesis because of a significant difference in the antifungal effect and mechanical properties between the 3D-printed denture base resin incorporating MPC and the 3D-printed denture base resin incorporating DDAM. Furthermore, the second null hypothesis was also rejected because even after thermocycling, the addition of MPC and DDAM negatively affected the mechanical properties of the 3D-printed denture base resin.

The FT-IR analysis revealed significant chemical interactions between PMMA and the additives MPC, DDAM, and their combination (MPC + DDAM). The addition of MPC resulted in shifts and intensity changes near the C=O stretching region ($\sim 1720 \text{ cm}^{-1}$) and introduced new vibrational modes in the 1000–1500 cm^{-1} range, likely due to interactions between MPC's phosphate groups and the PMMA matrix¹⁸. DDAM incorporation notably changed in the same regions, attributed to interactions involving its cationic and amine functional groups¹⁹.

When combining MPC and DDAM, the spectrum exhibited more complex changes, demonstrating synergistic interactions between the additives and PMMA²⁰. These modifications indicate the successful integration of the additives into the polymer matrix, altering its chemical structure and potentially enhancing its bioactivity. The observed chemical changes could play a key role in improving the antifungal and functional properties of the composite material.

Denture stomatitis is characterized by erythematous lesions on the oral mucosa, particularly on the palatal denture-bearing mucosa, caused by close prolonged contact with the removable denture²¹. Denture stomatitis

may occur due to factors such as inadequate oral hygiene, prolonged denture use, reduced salivary flow, and certain systemic conditions. However, the colonization of *C. albicans* biofilms is widely recognized as the primary cause of this fungal infection²². Developing 3D-printed denture base resins with antifungal properties that inhibit *C. albicans* biofilm formation is a promising approach to preventing denture stomatitis and improving oral health outcomes.

Several studies have revealed that hydrophilic surfaces effectively decrease protein adsorption and prevent bacterial biofilm formation. MPC, a methacrylate containing a phospholipid polar group in its side chain, is one of the most commonly used biocompatible and hydrophilic biomedical polymers^{23,24}. Incorporating MPC into 3D-printed denture base resins significantly reduced the adhesion of *C. albicans*. However, its impact on mechanical properties, particularly the flexural strength, must not be overlooked. Flexural strength is a critical property of the denture base resin, as it represents the primary mechanism behind clinical failures²⁵. Ensuring sufficient flexural strength is vital for the durability and functionality of denture bases under masticatory loads²⁶. Studies have demonstrated that incorporating hydrophilic and biocompatible polymers like MPC frequently results in a trade-off between antimicrobial properties and mechanical strength due to changes in the resin matrix structure²⁷.

Similarly, integrating QAMs, such as DDAM, into the resin matrix enhanced its antifungal properties by killing *C. albicans* through a contact-active mechanism²⁸. DDAM achieves this through its ability to disrupt microbial membranes via contact-killing²⁹. In our study, this bactericidal mechanism was further supported by the CLSM images, which revealed not only reduced fungal adhesion but also clear evidence of fungal cell death, particularly in the DDAM-containing groups. Among these, DDAM, a lipoid amine with a molecular weight of 631, has promising properties. It consists of two 18-carbon alkyl chains and two methyl groups attached to a positively charged quaternary ammonium structure. Gall first identified the antimicrobial and adjuvant properties of DDAM in a study examining over 100 chemical agents³⁰. However, this also decreased the flexural strength, which aligns with previous findings indicating that modifications to the resin composition can reduce the mechanical integrity³¹.

Thermocycling, performed for 10,000 cycles to simulate aging, revealed that while the antifungal efficacy slightly decreased due to aging, the antifungal activity was still maintained at significantly lower levels compared to the control in all experimental groups. Statistical analysis, including paired t-tests, revealed significant increases in CFU after-aging in all groups: control ($p=0.014$), 2% MPC ($p=0.001$), 2% DDAM ($p=0.003$), and 1% MPC + 1% DDAM ($p=0.003$) groups. However, the degree of increase varied among groups. Notably, the 1% MPC + 1% DDAM group demonstrated both antifungal efficacy and durability, showing the lowest CFU and relatively stable performance before- and after-aging.

Paired t-test results for flexural strength analysis after-aging showed significant reductions in the 2% MPC ($p=0.035$) and 2% DDAM ($p=0.021$) groups, whereas no significant differences were observed in the control ($p=0.210$) and 1% MPC + 1% DDAM groups ($p=0.525$). Such results of reduction in flexural strength are likely due to hydrothermal degradation and polymer network changes at higher levels of MPC or DDAM³². Although the 2% MPC group exhibited slightly higher flexural strength than the MPC + DDAM (M + D) group, the latter demonstrated markedly lower CFU, indicating superior antifungal performance, while the reduction of flexural strength was not significant compared to the 2% MPC or 2% DDAM group. Overall, the M + D group provided the most favorable balance between antifungal efficacy and mechanical durability.

Despite these challenges, the antifungal efficacy of MPC and QAM highlights the potential of these additives in improving the overall performance of denture base materials³³. However, further optimization of the MPC and QAM concentrations is required to achieve a balance between antimicrobial properties and mechanical strength. This could involve exploring alternative synthesis methods or using copolymers to mitigate the negative impact on the mechanical properties while preserving the strong antifungal effects.

In addition, the long-term effects of these modifications should be investigated under simulated oral conditions. The durability and functionality of modified denture bases are influenced by factors such as temperature fluctuations, pH variations, and enzymatic activity in the oral cavity. Future studies evaluating their performance *in vivo* will provide more comprehensive insights into their clinical applicability. Furthermore, expanding the scope to include patient-reported outcomes, such as comfort, esthetics, and wear resistance, will help determine the clinical value of these modified resins.

In conclusion, although incorporating MPC and DDAM into 3D-printed denture base resins is promising for addressing denture stomatitis challenges, further studies are required to optimize the material properties. Balancing antimicrobial efficacy with mechanical durability is critical for ensuring the success and sustainability of these innovations in prosthodontics.

Conclusions

The development of antimicrobial 3D-printed denture base materials incorporating MPC and DDAM has significant clinical implications. By reducing *C. albicans* colonization, these materials could decrease the prevalence of denture stomatitis, thereby improving the oral health and quality of life of denture wearers. Furthermore, the potential to reduce reliance on chemical denture cleansers or antifungal medications may enhance patient compliance and long-term cost-effectiveness.

Data availability

The datasets used and/or analyzed during the current study available from the corresponding author on reasonable request.

Received: 27 February 2025; Accepted: 6 October 2025

Published online: 12 November 2025

References

- Slade, G. D., Akinkugbe, A. A. & Sanders, A. E. Projections of US edentulism prevalence following 5 decades of decline. *J. Dent. Res.* **93**, 959–965 (2014).
- Al-Rafee, M. A. The epidemiology of edentulism and the associated factors: A literature review. *J. Family Med. Prim. Care* **9**, 1841–1843 (2020).
- Nagaraj, E., Mankani, N., Madalli, P. & Astekar, D. Socioeconomic factors and complete edentulism in north Karnataka population. *J. Indian Prosthodont. Soc.* **14**, 24–28 (2014).
- Alla, R., Raghavendra, K., Vyas, R. & Konakanchi, A. Conventional and contemporary polymers for the fabrication of denture prosthesis: Part I—overview, composition and properties. *Int. J. Appl. Dent. Sci.* **1**, 82–89 (2015).
- Frazer, R. Q., Byron, R. T., Osborne, P. B. & West, K. P. PMMA: an essential material in medicine and dentistry. *J. Long Term Eff. Med. Implants* **15**, 629–639 (2005).
- Matsuo, H. et al. Deterioration of polymethyl methacrylate dentures in the oral cavity. *Dent. Mater. J.* **34**, 234–239 (2015).
- Newton, A. Denture sore mouth. *Br. Dent. J.* **112**, 357–360 (1962).
- Yarborough, A. et al. Evidence regarding the treatment of denture stomatitis. *J. Prosthodont.* **25**, 288–301 (2016).
- Dar-Odeh, N. S., Al-Beyari, M. & Abu-Hammad, O. A. The role of antifungal drugs in the management of denture-associated stomatitis. *Int. Arabic J. Antimicrob. Agents* **2** (2012).
- Polychronakis, N. C., Polyzois, G. L., Lagouvardos, P. E. & Papadopoulos, T. D. Effects of cleansing methods on 3-D surface roughness, gloss and color of a polyamide denture base material. *Acta Odontol. Scand.* **73**, 353–363 (2015).
- Guazzo, R. et al. Graphene-based nanomaterials for tissue engineering in the dental field. *Nanomaterials* **8**, 349 (2018).
- Donlan, R. M. & Costerton, J. W. Biofilms: survival mechanisms of clinically relevant microorganisms. *Clin. Microbiol. Rev.* **15**, 167–193 (2002).
- Bajunaid, S. O., Baras, B. H., Balhaddad, A. A., Weir, M. D. & Xu, H. H. Antibiofilm and protein-repellent polymethylmethacrylate denture base acrylic resin for treatment of denture stomatitis. *Materials* **14**, 1067 (2021).
- Ishihara, K., Ueda, T. & Nakabayashi, N. Preparation of phospholipid polymers and their properties as polymer hydrogel membranes. *Polym. J.* **22**, 355–360 (1990).
- Zhang, N., Weir, M. D., Romberg, E., Bai, Y. & Xu, H. H. Development of novel dental adhesive with double benefits of protein-repellent and antibacterial capabilities. *Dent. Mater.* **31**, 845–854 (2015).
- Allaker, R. P. The use of nanoparticles to control oral biofilm formation. *J. Dent. Res.* **89**, 1175–1186 (2010).
- Zhang, N. et al. Novel dental cement to combat biofilms and reduce acids for orthodontic applications to avoid enamel demineralization. *Materials* **9**, 413 (2016).
- Smith, B. Infrared spectroscopy of polymers. X: polyacrylates (2023).
- Mushtaq, S., Ahmad, N. M., Mahmood, A. & Iqbal, M. Antibacterial amphiphilic copolymers of dimethylamino ethyl methacrylate and methyl methacrylate to control biofilm adhesion for antifouling applications. *Polymers* **13**, 216 (2021).
- Cao, L. et al. Novel protein-repellent and antibacterial polymethyl methacrylate dental resin in water-aging for 6 months. *BMC Oral Health* **22**, 457 (2022).
- Davenport, J. C. The oral distribution of candida in denture stomatitis. *Br. Dent. J.* **129**, 151–156 (1970).
- Ramage, G., Tomsett, K., Wickes, B. L., López-Ribot, J. L. & Redding, S. W. Denture stomatitis: a role for Candida biofilms. *Oral Surg. Oral Med. Oral Pathol. Oral Radiol. Endod. Dent.* **98**, 53–59 (2004).
- Nakabayashi, N. & Iwasaki, Y. Copolymers of 2-methacryloyloxyethyl phosphorylcholine (MPC) as biomaterials. *Bio-Med. Mater. Eng.* **14**, 345–354 (2004).
- Müller, R. et al. Influences of protein films on antibacterial or bacteria-repellent surface coatings in a model system using silicon wafers. *Biomaterials* **30**, 4921–4929 (2009).
- Alshaikh, A. A. et al. 3D-printed nanocomposite denture-base resins: effect of ZrO₂ nanoparticles on the mechanical and surface properties in vitro. *Nanomaterials* **12**, 2451 (2022).
- Gad, M. M., Al-Thobity, A. M., Fouad, S. M., Närpäkangas, R. & Raustia, A. Flexural and surface properties of PMMA denture base material modified with thymoquinone as an antifungal agent. *J. Prosthodont.* **29**, 243–250 (2020).
- Cherchali, F. Z. et al. Effectiveness of the DHMAI monomer in the development of an antibacterial dental composite. *Dent. Mater.* **33**, 1381–1391 (2017).
- Liu, S. Y. et al. Antimicrobial activity of a quaternary ammonium methacryloxy silicate-containing acrylic resin: a randomised clinical trial. *Sci. Rep.* **6**, 21882 (2016).
- Makvandi, P., Jamaledin, R., Jabbari, M., Nikfarjam, N. & Borzacchiello, A. Antibacterial quaternary ammonium compounds in dental materials: A systematic review. *Dent. Mater.* **34**, 851–867 (2018).
- Gall, D. The adjuvant activity of aliphatic nitrogenous bases. *Immunology* **11**, 369–386 (1966).
- AlAzzam, N. F. et al. The effect of incorporating dimethylaminohexadecyl methacrylate and/or 2-methacryloyloxyethyl phosphorylcholine on flexural strength and surface hardness of heat polymerized and 3D-printed denture base materials. *Materials* **17**, 4625 (2024).
- Ayaz, E. A., Bağış, B. & Turgut, S. Effects of thermal cycling on surface roughness, hardness and flexural strength of polymethylmethacrylate and polyamide denture base resins. *J. Appl. Biomater. Funct. Mater.* **13**, e280–e286 (2015).
- Bajunaid, S. O., Baras, B. H., Weir, M. D. & Xu, H. H. Denture acrylic resin material with antibacterial and protein-repelling properties for the prevention of denture stomatitis. *Polymers Dent.* **14**, 230 (2022).

Acknowledgements

This work was supported by the National Research Foundation of Korea (NRF) grant funded by the Korean government (MSIT) (No. 2022R1C1C1010304)

Author contributions

S.E.L. and J.S.K. conceived and designed the experiments. S.E.L. conducted all the experiments. S.E.L. and J.S.K. interpreted and analyzed the data. S.E.L. conceived the study and wrote the manuscript. J.S.K. provided manuscript writing assistance and critically revised the manuscript, adding important intellectual content. All authors reviewed and approved the final manuscript.

Declarations

Competing interests

The authors declare no competing interests.

Additional information

Correspondence and requests for materials should be addressed to J.-S.K.

Reprints and permissions information is available at www.nature.com/reprints.

Publisher's note Springer Nature remains neutral with regard to jurisdictional claims in published maps and institutional affiliations.

Open Access This article is licensed under a Creative Commons Attribution-NonCommercial-NoDerivatives 4.0 International License, which permits any non-commercial use, sharing, distribution and reproduction in any medium or format, as long as you give appropriate credit to the original author(s) and the source, provide a link to the Creative Commons licence, and indicate if you modified the licensed material. You do not have permission under this licence to share adapted material derived from this article or parts of it. The images or other third party material in this article are included in the article's Creative Commons licence, unless indicated otherwise in a credit line to the material. If material is not included in the article's Creative Commons licence and your intended use is not permitted by statutory regulation or exceeds the permitted use, you will need to obtain permission directly from the copyright holder. To view a copy of this licence, visit <http://creativecommons.org/licenses/by-nc-nd/4.0/>.

© The Author(s) 2025